AD-A062 621   RENSSELAER POLYTECHNIC INST TROY N Y DEPT OF MECHANI--ETC   F/G 9/1
AN ANALYSIS OF CONTOURED CRYSTAL RESONATORS OPERATING IN OVERTO--ETC(U)
NOV 78   H F TIERSTEN, R C SMYTHE   N00014-76-C-0368

UNCLASSIFIED   TR-26   NL

| OF |
ADA
062621

END
DATE
FILMED
3 -79
DDC

(12) LEVEL II

Rensselaer Polytechnic Institute
Troy, New York 12181

AN ANALYSIS OF CONTOURED CRYSTAL RESONATORS OPERATING IN OVERTONES OF COUPLED THICKNESS-SHEAR AND THICKNESS-TWIST

by

H.F. Tiersten and R.C. Smythe

Office of Naval Research
Contract N00014-76-C-0368
Project NR 318-009
Technical Report No. 26

November 1978

Rensselaer Polytechnic Institute

Troy, New York 12181

(6) AN ANALYSIS OF CONTOURED CRYSTAL RESONATORS OPERATING IN OVERTONES OF COUPLED THICKNESS-SHEAR AND THICKNESS-TWIST

by

(10) H.F. Tiersten ~~and~~ R.C. Smythe

(9) Technical rept.

(12) 25 p.

(14) TR-26

(15)
Office of Naval Research
Contract N00014-76-C-0368, DAAG29-76-G-0176
Project NR 318-009
Technical Report No. 26

(11) November 1978

409 359

SECURITY CLASSIFICATION OF THIS PAGE (When Data Entered)

REPORT DOCUMENTATION PAGE		READ INSTRUCTIONS BEFORE COMPLETING FORM
1. REPORT NUMBER No. 26	2. GOVT ACCESSION NO.	3. RECIPIENT'S CATALOG NUMBER
4. TITLE (and Subtitle) AN ANALYSIS OF CONTOURED CRYSTAL RESONATORS OPERATING IN OVERTONES OF COUPLED THICKNESS-SHEAR AND THICKNESS-TWIST		5. TYPE OF REPORT & PERIOD COVERED Technical Report 6. PERFORMING ORG. REPORT NUMBER
7. AUTHOR(s) H.F. Tiersten and R.C. Smythe		8. CONTRACT OR GRANT NUMBER(s) N00014-76-C-0368
9. PERFORMING ORGANIZATION NAME AND ADDRESS Department of Mechanical Engineering, Aeronautical Engineering and Mechanics Rensselaer Polytechnic Institute Troy, New York 12181		10. PROGRAM ELEMENT, PROJECT, TASK AREA & WORK UNIT NUMBERS NR 318-009
11. CONTROLLING OFFICE NAME AND ADDRESS Office of Naval Research Physics Branch Washington, D.C. 20360		12. REPORT DATE November 1978 13. NUMBER OF PAGES 22
14. MONITORING AGENCY NAME & ADDRESS(if different from Controlling Office)		15. SECURITY CLASS. (of this report) Unclassified 15a. DECLASSIFICATION/DOWNGRADING SCHEDULE

16. DISTRIBUTION STATEMENT (of this Report)

Distribution of this document is unlimited.

DISTRIBUTION STATEMENT A
Approved for public release;
Distribution Unlimited

17. DISTRIBUTION STATEMENT (of the abstract entered in Block 20, if different from Report)

18. SUPPLEMENTARY NOTES

19. KEY WORDS (Continue on reverse side if necessary and identify by block number)

Piezoelectricity	Precision Oscillators
Elasticity	Trapped Energy
Plate Vibrations	Thickness-Shear
Quartz Resonators	Thickness-Twist
Contoured Resonators	Overtones

20. ABSTRACT (Continue on reverse side if necessary and identify by block number)

A previous treatment of overtone modes in trapped energy resonators is extended to the case of plates with slowly varying thickness. The resulting single scalar equation is applied in the analysis of plano-convex contoured quartz crystal resonators and a lumped parameter representation of the admittance, which is valid in the vicinity of a resonance, is obtained. The analysis holds for the fundamental and anharmonic overtones of the fundamen- and each harmonic overtone thickness mode. The influence of piezoelectric cont'

DD FORM 1 JAN 73 1473 EDITION OF 1 NOV 65 IS OBSOLETE
S/N 0102-014-6601

Unclassified
SECURITY CLASSIFICATION OF THIS PAGE (When Data Entered)

78 12 18 046

Unclassified

SECURITY CLASSIFICATION OF THIS PAGE(When Data Entered)

CONT

stiffening, electrode mass loading and electrical shorting is included in the analysis. No adjustable parameters are required in the theory. Although the basic piezoelectric differential equation employed here is quite different from the ones that have been employed in similar applications heretofore, the analysis accounting for the contouring has appeared in the literature. It is shown that calculations based on the analysis agree extremely well with experimental results obtained with contoured AT-cut quartz crystal resonators.

Unclassified

SECURITY CLASSIFICATION OF THIS PAGE(When Data Entered)

AN ANALYSIS OF CONTOURED CRYSTAL RESONATORS OPERATING IN OVERTONES OF COUPLED THICKNESS-SHEAR AND THICKNESS-TWIST

H.F. Tiersten
Department of Mechanical Engineering,
Aeronautical Engineering & Mechanics
Rensselaer Polytechnic Institute
Troy, New York 12181

R.C. Smythe
Piezo Technology Incorporated
Orlando, Florida 32804

ABSTRACT

A previous treatment of overtone modes in trapped energy resonators is extended to the case of plates with slowly varying thickness. The resulting single scalar equation is applied in the analysis of plano-convex contoured quartz crystal resonators and a lumped parameter representation of the admittance, which is valid in the vicinity of a resonance, is obtained. The analysis holds for the fundamental and anharmonic overtones of the fundamental and each harmonic overtone thickness mode. The influence of piezoelectric stiffening, electrode mass loading and electrical shorting is included in the analysis. No adjustable parameters are required in the theory. Although the basic piezoelectric differential equation employed here is quite different from the ones that have been employed in similar applications heretofore, the analysis accounting for the contouring has appeared in the literature. It is shown that calculations based on the analysis agree extremely well with experimental results obtained with contoured AT-cut quartz crystal resonators.

1. Introduction

In a recent investigation[1] the three-dimensional equations of linear piezoelectricity, with the aid of certain simplifying assumptions, were applied in the analysis of rotated Y-cut quartz trapped energy resonators with rectangular electrodes operating in overtones of coupled thickness-shear and thickness-twist vibrations. In this paper the previous analysis is extended to the case of plates with slowly varying thickness. The asymptotic dispersion relation for small wavenumbers along the electroded flat plate obtained in the recent analysis[1] of trapped energy resonators enables us to construct the single scalar differential equation of coupled thickness-shear and thickness-twist, which holds for plates with slowly varying thickness. The simplifying assumptions of small piezoelectric coupling, one-dimensional (thickness) dependence of all electrical variables and the neglect of certain small unimportant elastic constants employed in the earlier[1] analysis naturally are employed here also. The influence of piezoelectric stiffening, electrode mass loading and electrical shorting is included nonetheless. Since the influence of the contouring on the trapping is much greater than the influence of the discontinuity between the electroded and unelectroded region, the edge of the electrode is ignored in the determination of the eigensolution. Since the mode is assumed to be highly trapped in the vicinity of the center of the contoured plate, the boundary conditions at the edge of the plate are ignored in the analysis. The procedure for obtaining the eigensolution follows that of Wilson[2], who treated the purely elastic case using an incorrect equation which had been used earlier by others[3,4].

The resulting inhomogeneous single scalar equation is applied in the analysis of the forced vibrations of a plano-convex contoured AT-cut quartz crystal resonator and a lumped parameter representation of the admittance is obtained. Calculations based on the analysis are in excellent agreement with the results of experiments on contoured AT-cut quartz crystal resonators.

2. Basic Equations

A schematic diagram of a plano-convex quartz crystal resonator is shown in Fig.1. Since the thickness h is a slowly varying function of x_1 and x_3, it is appropriate to first consider the solution for the electroded flat plate shown in Fig.2 and then generalize it to be applicable to the contoured plate with slowly varying thickness. Accordingly, we first briefly reproduce the analysis[1] of the electroded flat plate. On the basis of the simplifying assumptions of small piezoelectric coupling, the neglect of certain relatively small unimportant elastic constants and the fact that in the essentially thickness-shear modes of interest, the wavenumbers in both the x_1- and x_3-directions are much smaller than the thickness wavenumber, it has been shown[1] that to second order in small quantities the differential equations that remain to be satisfied take the form

$$c_{11}u_{1,11} + (c_{12} + c_{66})u_{2,12} + c_{66}u_{1,22} + c_{55}u_{1,33} + e_{26}\varphi_{,22} = \rho\ddot{u}_1,$$

$$(c_{66} + c_{12})u_{1,12} + c_{66}u_{2,11} + c_{22}u_{2,22} = \rho\ddot{u}_2,$$

$$e_{26}u_{1,22} - \epsilon_{22}\varphi_{,22} = 0, \tag{2.1}$$

and we note that the notation is defined in Ref.1. We further note that for the circumstances outlined it has been shown[1] that u_3 is two orders of magnitude smaller than u_1 and, hence, negligible to the order of approximation being obtained. To the same order of approximation the pertinent constitutive equations take the form[1]

$$T_{21} = c_{66}(u_{1,2} + u_{2,1}) + e_{26}\varphi_{,2},$$

$$T_{22} = c_{12}u_{1,1} + c_{22}u_{2,2}, \quad T_{11} = c_{11}u_{1,1} + c_{12}u_{2,2},$$

$$T_{31} = c_{55}u_{1,3} + e_{25}\varphi_{,2}, \quad D_2 = e_{26}u_{1,2} - \epsilon_{22}\varphi_{,2}, \tag{2.2}$$

and the boundary conditions that remain to be satisfied on the electroded major surfaces of the flat plate take the form

$$T_{21} = \mp 2\rho' h' \ddot{u}_1, \quad T_{22} = \mp 2\rho' h' \ddot{u}_2, \quad \varphi = \pm (V/2)e^{i\omega t} \quad \text{at } x_2 = \pm h, \tag{2.3}$$

where ρ' is the mass density of the electrode plating.

It has been shown[1,5] that in order to remove the inhomogeneous driving term from the boundary condition $(2.3)_3$ and place it in the differential equation $(2.1)_1$, we take

$$u_1 = \hat{u}_1 + Kx_2 e^{i\omega t}, \quad u_2 = \hat{u}_2,$$

$$\varphi = \frac{Vx_2}{2h} e^{i\omega t} + \frac{e_{26}}{\epsilon_{22}} \hat{u}_1 + Cx_2 e^{i\omega t}, \tag{2.4}$$

where

$$K = -e_{26}V/c_{66}2h, \quad C = -(e_{26}/\epsilon_{22})\hat{u}_1(h)/h. \tag{2.5}$$

Then the substitution of (2.4) into (2.1) and (2.3), with (2.2) and (2.5), yields

$$c_{11}\hat{u}_{1,11} + (c_{12} + c_{66})\hat{u}_{2,12} + \bar{c}_{66}\hat{u}_{1,22} + c_{55}\hat{u}_{1,33} = \rho\ddot{\hat{u}}_1 - \rho\omega^2 Kx_2 e^{i\omega t},$$

$$c_{66}\hat{u}_{2,11} + (c_{12} + c_{66})\hat{u}_{1,12} + c_{22}\hat{u}_{2,22} = \rho\ddot{\hat{u}}_2, \tag{2.6}$$

$$c_{66}\hat{u}_{2,1} + \bar{c}_{66}\hat{u}_{1,2} \mp (e_{26}^2/\epsilon_{22}h)\hat{u}_1 = \mp 2\rho' h' \ddot{\hat{u}}_1 \quad \text{at } x_2 = \pm h,$$

$$c_{22}\hat{u}_{2,2} + c_{12}\hat{u}_{1,1} = \mp 2\rho' h' \ddot{\hat{u}}_2 \quad \text{at } x_2 = \pm h, \tag{2.7}$$

where

$$\bar{c}_{66} = c_{66} + e_{26}^2/\epsilon_{22}, \tag{2.8}$$

and $(2.1)_3$ and $(2.3)_3$ are satisfied by the forms chosen. Equations (2.6) and (2.7) constitute a system of linear inhomogeneous differential equations with homogeneous boundary conditions on the major surfaces of the electroded flat plate. It has been shown[1,5] that an asymptotic eigensolution for plate waves valid to second order in the small wavenumbers ξ and ν along the electroded flat plate can be written in the form

$$\hat{u}_1 = (B_1^{(1)} \sin \eta_1 x_2 + B_1^{(2)} \sin \varkappa\eta_1 x_2) \cos \xi x_1 \cos \nu x_3 e^{i\tilde{\omega}t} ,$$

$$\hat{u}_2 = (B_2^{(1)} \cos \eta_1 x_2 + B_2^{(2)} \cos \varkappa\eta_1 x_2) \sin \xi x_1 \cos \nu x_3 e^{i\tilde{\omega}t} , \tag{2.9}$$

where

$$\eta_1 = \frac{n\pi}{2h} , \quad \varkappa = \sqrt{\frac{\bar{c}_{66}}{c_{22}}} , \quad B_2^{(1)} = \frac{r\xi B_1^{(1)}}{\eta_1} , \quad B_1^{(2)} = - \frac{r\xi B_2^{(2)}}{\varkappa\eta_1} ,$$

$$r = \frac{c_{12} + c_{66}}{\bar{c}_{66} - c_{22}} , \quad B_2^{(2)} = \frac{(-1)^{\frac{n+1}{2}} (c_{12} + rc_{22})\xi B_1^{(1)}}{c_{22}\varkappa\eta_1 \sin \varkappa\eta_1 h} , \tag{2.10}$$

provided the dispersion relation

$$M_n\xi^2 + c_{55}\nu^2 + \frac{n^2\pi^2}{4h^2} \hat{c}_{66} - \rho\tilde{\omega}^2 = 0 , \tag{2.11}$$

which is valid to second order in ξ and ν, is satisfied, and where we have employed the definitions

$$M_n = c_{11} + (c_{12} + c_{66})r + 4 \frac{(r\bar{c}_{66} - c_{66})(c_{22}r + c_{12})\cot \varkappa n\pi/2}{c_{22}n\pi\varkappa} ,$$

$$\hat{c}_{66} = \bar{c}_{66}\left(1 - \frac{8k_{26}^2}{n^2\pi^2} - 2\hat{R}\right), \quad k_{26}^2 = \frac{e_{26}^2}{\bar{c}_{66}\epsilon_{22}} , \quad \hat{R} = \frac{2\rho' h'}{\rho h} . \tag{2.12}$$

The derivation of the dispersion relation (2.11) in Refs. 1 and 5 reveals that (2.11) is obtained from the homogeneous form of $(2.6)_1$ when $(2.6)_2$ and (2.7) are satisfied to second order in ξ and ν. In particular, when $(2.6)_2$ and (2.7) are satisfied to second order in ξ and ν and the resulting relations are substituted in the homogeneous form of $(2.6)_1$, there results

$$\left(M_n\xi^2 + c_{55}\nu^2 + \frac{n^2\pi^2}{4h^2} \hat{c}_{66} - \rho\tilde{\omega}^2\right)\hat{u}_1 = 0 , \tag{2.13}$$

from which the dispersion relation (2.11) is obtained for nonzero $\hat{u}_1$, which is the large mechanical displacement field. On account of the foregoing, from $(2.6)_1$, $(2.5)_1$ and (2.13) it is clear that the inhomogeneous differential equation governing coupled thickness-shear and thickness-twist vibrations is of the form

$$M_n \frac{\partial^2 \hat{u}_1}{\partial x_1^2} + c_{55} \frac{\partial^2 \hat{u}_1}{\partial x_3^2} - \frac{n^2 \pi^2}{4h^2} \hat{c}_{66} \hat{u}_1 - \rho \ddot{\hat{u}}_1 = \rho \omega^2 \frac{e_{26} V x_2}{c_{66} 2h} e^{i\omega t} , \tag{2.14}$$

where ω is the driving frequency. Clearly, the homogeneous $(V = 0)$ solutions for the flat plate are consistent with (2.11). It has been shown[1,5] that when the approximation holds and, hence, by virtue of the foregoing, Eq. (2.14) may be employed, the approximate edge conditions to be satisfied at a junction between an electroded and unelectroded region of the plate are the continuity of

$$\hat{u}_1 \text{ and } \partial \hat{u}_1 / \partial n , \tag{2.15}$$

where n represents the normal to the junction.

We now generalize Eq. (2.14) for the flat plate to be applicable to a contoured plate with slowly varying thickness simply by permitting h in (2.14) to be a slowly varying function of x_1 and x_3. To this end consider the geometry shown in Fig. 3. Since, as shown in Fig. 3, the triangle inscribed in the semicircle and containing a diameter is a right triangle, all three right triangles are similar and we have

$$\frac{2R - (2h_o - 2h)}{r} = \frac{r}{2h_o - 2h} , \tag{2.16}$$

where

$$r = (x_1^2 + x_3^2)^{\frac{1}{2}} , \tag{2.17}$$

and R is the radius of curvature of the spherical surface of the contoured resonator. Since $2h_o \ll R$, from (2.16) with (2.17), we obtain

$$2h = 2h_o[1 - (x_1^2 + x_3^2)/4Rh_o] , \tag{2.18}$$

the substitution of which in (2.14) and expansion to first order in $x_1^2 + x_3^2$ yields

$$M_n \frac{\partial^2 \hat{u}_1}{\partial x_1^2} + c_{55} \frac{\partial^2 \hat{u}_1}{\partial x_3^2} - \frac{n^2 \pi^2 \hat{c}_{66}}{4h_o^2} \left[1 + \frac{(x_1^2 + x_3^2)}{2Rh_o}\right] \hat{u}_1 - \rho\ddot{\hat{u}}_1 = \rho\omega^2 \frac{e_{26} V x_2}{c_{66} 2h} e^{i\omega t} , \tag{2.19}$$

which is the inhomogeneous differential equation for coupled thickness-shear and thickness-twist vibrations of a plano-convex resonator.

3. Contoured Resonator

The problem of a contoured resonator driven into coupled thickness-shear and thickness-twist vibrations by the application of a driving voltage across the electrodes in the steady state may now be treated by finding the steady-state solution of (2.19) which remains bounded and vanishes at infinity. The solution is assumed to be continuous across the edge of the electrode because the influence of the contouring on the mode shape (trapping) is much greater than the influence of the discontinuity between the electroded and unelectroded region. The differential equation of coupled thickness-shear and thickness-twist vibrations for the electroded portion of the contoured resonator, Eq. (2.19), is employed because the modes are sharply confined in the vicinity of the center of the contoured resonator and the relatively large electrodes are located in the central part of the contoured plate. Similarly, the boundary conditions at the edge of the contoured plate are ignored in the analysis because the modes are highly trapped in the vicinity of the center of the contoured plate and have negligible amplitude at the edge of the plate.

We first seek the eigensolutions of the associated homogeneous problem, i.e., with $V = 0$. To this end we take the $\hat{u}_1$-displacement field in the form

$$\hat{u}_1(x_1, x_2, x_3, t) = u(x_1, x_3)\ \sin(n\pi x_2/2h)e^{i\tilde{\omega}t}\ , \tag{3.1}$$

the substitution of which in (2.19) yields

$$M_n \frac{\partial^2 u}{\partial x_1^2} + c_{55}\frac{\partial^2 u}{\partial x_3^2} - \frac{n^2\pi^2\hat{c}_{66}}{4h_o^2}\left[1 + \frac{(x_1^2 + x_3^2)}{2Rh_o}\right] u + \rho\tilde{\omega}^2 u = 0\ , \tag{3.2}$$

where $\tilde{\omega}$ denotes the eigenfrequency. As a solution of (3.2) we take

$$u = X(x_1)Z(x_3)\ , \tag{3.3}$$

which satisfies (3.2) provided

$$X'' + (\gamma^2 - \alpha_n^2 x_1^2)X = 0\ , \quad Z'' + (\mu^2 - \beta_n^2 x_3^2)Z = 0\ , \tag{3.4}$$

where the undetermined separation constants γ and μ satisfy

$$\rho\tilde{\omega}^2 - \frac{n^2\pi^2}{4h_o^2}\hat{c}_{66} = M_n\gamma^2 + c_{55}\mu^2\ , \tag{3.5}$$

and

$$\alpha_n^2 = n^2\pi^2\hat{c}_{66}/8Rh_o^3 M_n\ , \quad \beta_n^2 = n^2\pi^2\hat{c}_{66}/8Rh_o^3 c_{55}\ . \tag{3.6}$$

The only solutions of (3.4) that are bounded for all x_1 and x_3 and vanish at ∞ are the Hermite functions[6]

$$X_{mn} = e^{-\alpha_n \frac{x_1^2}{2}} H_m(\sqrt{\alpha_n}x_1)\ , \quad Z_{pn} = e^{-\frac{\beta_n x_3^2}{2}} H_p(\sqrt{\beta_n}x_3)\ , \tag{3.7}$$

where H_m and H_p are Hermite polynomials and

$$\gamma_{mn}^2 = \alpha_n(1 + 2m)\ , \quad \mu_{pn}^2 = \beta_n(1 + 2p)\ , \tag{3.8}$$

which are determined from the condition that the series for H_m and H_p terminate and they be polynomials. Since we are interested in only those solutions which are symmetric in x_1 and x_3, we have

$$m, p = 0, 2, 4 \ldots . \tag{3.9}$$

For a given value of n, m and p, (3.8), with (3.6), determines the values of the separation constants γ_{mn} and μ_{pn}, which, from (3.5), yield the eigenfrequencies $\tilde{\omega}_{nmp}$ in the form

$$\tilde{\omega}^2_{nmp} = \frac{n^2\pi^2\hat{c}_{66}}{4h_o^2\rho}\left[1 + \frac{1}{n\pi}\sqrt{\frac{2h_o}{R}}\left(\sqrt{\frac{M_n}{\hat{c}_{66}}}\,(2m+1) + \sqrt{\frac{c_{55}}{\hat{c}_{66}}}\,(2p+1)\right)\right]. \tag{3.10}$$

We now write the steady-state solution of (2.19) as a sum of eigensolutions, thus

$$\hat{u}_1 = e^{i\omega t}\sum_n\sum_m\sum_p H^{nmp}\tilde{u}_{1nmp}, \tag{3.11}$$

where

$$\hat{u}_{1nmp} = \tilde{u}_{1nmp}e^{i\tilde{\omega}_{nmp}t}, \quad \tilde{u}_{1nmp} = \sin\frac{n\pi x_2}{2h}\,u_{nmp}, \tag{3.12}$$

and

$$u_{nmp} = e^{-\alpha_n\frac{x_1^2}{2}}H_m(\sqrt{\alpha_n}\,x_1)\,e^{-\beta_n\frac{x_3^2}{2}}H_p(\sqrt{\beta_n}\,x_3), \tag{3.13}$$

and we note that along with $\hat{u}_1$, from $(2.4)_3$ and $(2.5)_2$, we have

$$\varphi = \frac{Vx_2}{2h}e^{i\omega t} + \frac{e_{26}}{\epsilon_{22}}\sum_n\sum_m\sum_p H^{nmp}u_{nmp}\left(\sin\frac{n\pi x_2}{2h} - (-1)^{\frac{n-1}{2}}\frac{x_2}{h}\right)e^{i\omega t}. \tag{3.14}$$

Since the eigensolutions are sharply confined in the vicinity of the center of the contoured plate and have negligible amplitudes at relatively small values of x_1 and x_3, 2h in (2.18) may be replaced by $2h_o$ in any integration over the eigensolutions performed in the course of this forced vibration analysis without appreciable error. When h is replaced by h_o, the solution functions in $(3.12)_2$ with (3.13) satisfy an orthogonality condition, which may be written in the form[7]

$$\int_{-\infty}^{\infty}\int_{-\infty}^{\infty}\int_{-h_o}^{h_o} \tilde{u}_{1nmp}\tilde{u}_{1\nu\mu\tau}\, dx_1 dx_3 dx_2 = L_{(n)(m)(p)}\delta_{n\nu}\delta_{m\mu}\delta_{p\tau} , \tag{3.15}$$

where

$$L_{nmp} = \pi h_o 2^m m!\, 2^p p!/\sqrt{\alpha_n}\,\sqrt{\beta_n} . \tag{3.16}$$

Substituting from (3.11) and (3.12) into (2.19) and employing (3.2) for each nmp-eigensolution, we obtain

$$\sum_n \sum_m \sum_p H^{nmp}(\omega^2 - \tilde{\omega}^2_{nmp}) \sin\frac{n\pi x_2}{2h}\, u_{nmp} = \frac{\omega^2 e_{26} V x_2}{c_{66} 2h} , \tag{3.17}$$

where it is understood that $V = 0$ in the unelectroded region. From (3.17) we form

$$\sum_n \sum_m \sum_p H^{nmp}(\omega^2 - \tilde{\omega}^2_{nmp}) \int_{-\infty}^{\infty}\int_{-\infty}^{\infty} u_{nmp}u_{\nu\mu\tau}dx_1\, dx_3 \int_{-h}^{h} \sin\frac{n\pi x_2}{2h}\sin\frac{\nu\pi x_2}{2h}\, dx_2 =$$

$$\frac{\omega^2 e_{26} V}{2c_{66}} \int_{A_e} \frac{1}{h}\, u_{\nu\mu\tau}\, dx_1 dx_3 \int_{-h}^{h} x_2 \sin\frac{\nu\pi x_2}{2h}\, dx_2 , \tag{3.18}$$

where A_e is the area of the electrode, and replacing h by h_o on both sides of (3.18), with the aid of the orthogonality condition in (3.15), we find

$$H^{nmp} = \frac{(-1)^{\frac{n-1}{2}} e_{26} 4h_o \mathcal{J}_{nmp} V}{c_{66} n^2 \pi^2 L_{nmp}[1 - (\tilde{\omega}^2_{nmp}/\omega^2)]} , \tag{3.19}$$

where

$$\mathcal{J}_{nmp} = 4F_{1nm}F_{3np} , \tag{3.20}$$

and if, as is reasonable in the case of the contoured resonator because the mode shape is sharply confined to the center, we replace the circular electrode by the circumscribed square with lengths $2\ell_1 = 2\ell_3$, we have

$$F_{1nm} = \int_0^{\ell_1} e^{-\alpha_n \frac{x_1^2}{2}} H_m(\sqrt{\alpha_n}\, x_1)\, dx_1 ,$$

$$F_{3np} = \int_0^{\ell_3} e^{-\beta_n \frac{x_3^2}{2}} H_p(\sqrt{\beta_n}\, x_3)\, dx_3 . \tag{3.21}$$

Thus, Eqs. (2.4), (2.5), (3.11) - (3.14), (3.16) and (3.19) - (3.21) constitute the series representation of the steady-state solution for the linear forced vibrations of this contoured resonator. In the vicinity of a resonance, say the NMPth, one term in the sums in (3.11) and (3.14) dominates and the others are negligible. Thus in the vicinity of said resonance the steady-state solution may be written

$$u_1 = H^{NMP} \sin \frac{N\pi x_2}{2h}\, u_{NMP} e^{i\omega t} - \frac{e_{26} V x_2}{c_{66} 2h} e^{i\omega t} ,$$

$$\varphi = \frac{V x_2}{2h} e^{i\omega t} + \frac{e_{26}}{\epsilon_{22}} H^{NMP} u_{NMP}\left(\sin \frac{N\pi x_2}{2h} - (-1)^{\frac{N-1}{2}} \frac{x_2}{h}\right) e^{i\omega t} , \tag{3.22}$$

where, as usual, $\tilde{\omega}_{NMP}$ in (3.22) is to be replaced by

$$\hat{\omega}_{NMP} = \tilde{\omega}_{NMP} + i\tilde{\omega}_{NMP}/2Q_{NMP} , \tag{3.23}$$

in which Q_{NMP} is the unloaded quality factor of the contoured resonator in the NMPth mode. The admittance Y_{NMP} of this rotated Y-cut contoured resonator operating in the NMPth mode is obtained by substituting from (3.22) into $(2.2)_5$, which is then substituted into

$$I = - \int_{A_e} \dot{D}_2\, dx_1 dx_3 , \tag{3.24}$$

with the result

$$Y_{NMP} = \frac{I}{V} = \frac{i\omega\epsilon_{22}}{2h} (1 + \hat{k}_{26}^2)\hat{A}_e + \frac{i\omega\epsilon_{22}\hat{k}_{26}^2 4\mathcal{J}_{NMP}^2}{[(\tilde{\omega}_{NMP}^2/\omega^2) - 1] N^2 \pi^2 L_{NMP}} , \tag{3.25}$$

where

$$\hat{k}_{26}^2 = e_{26}^2/c_{66}\varepsilon_{22}\,, \quad \hat{A}_e = A_e(1 + \ell_1^2/8Rh_o)\,, \tag{3.26}$$

and in obtaining the second term in (3.25) we have again replaced the circular electrode by the circumscribed square with lengths $2\ell_1 = 2\ell_3$ to perform the integrations. The quantities C_o and C_{1NMP} defined by

$$C_o = \frac{\hat{A}_e\varepsilon_{22}(1+\hat{k}_{26}^2)}{2h_o}\,, \quad C_{1NMP} = \frac{4\varepsilon_{22}\hat{k}_{26}^2\mathcal{J}_{NMP}^2}{N^2\pi^2 L_{NMP}}\,, \tag{3.27}$$

are called the static and motional capacitances, respectively. The integrals appearing in (3.21), which appear prominently in $(3.27)_2$, have been evaluated for a few values of M and P and take the form

$$F_{1N0} = \frac{1}{\sqrt{\alpha_N}}\sqrt{\frac{\pi}{2}}\,\mathrm{erf}\sqrt{\frac{\alpha_N}{2}}\,\ell_1\,, \quad F_{3N0} = \frac{1}{\sqrt{\beta_N}}\sqrt{\frac{\pi}{2}}\,\mathrm{erf}\sqrt{\frac{\beta_N}{2}}\,\ell_3\,,$$

$$F_{1N2} = \frac{2}{\sqrt{\alpha_N}}\sqrt{\frac{\pi}{2}}\,\mathrm{erf}\sqrt{\frac{\alpha_N}{2}}\,\ell_1 - 4\ell_1\,e^{-\alpha_N\ell_1^2/2}\,,$$

$$F_{3N2} = \frac{2}{\sqrt{\beta_N}}\sqrt{\frac{\pi}{2}}\,\mathrm{erf}\sqrt{\frac{\beta_N}{2}}\,\ell_3 - 4\ell_3\,e^{-\beta_N\ell_3^2/2}\,,$$

$$F_{1N4} = \frac{12}{\sqrt{\alpha_N}}\sqrt{\frac{\pi}{2}}\,\mathrm{erf}\sqrt{\frac{\alpha_N}{2}}\,\ell_1 - 16\,\alpha_N\ell_1^3e^{-\alpha_N\ell_1^2/2}\,,$$

$$F_{3N4} = \frac{12}{\sqrt{\beta_N}}\sqrt{\frac{\pi}{2}}\,\mathrm{erf}\sqrt{\frac{\beta_N}{2}}\,\ell_3 - 16\,\beta_N\,\ell_3^3e^{-\beta_N\ell_3^2/2}\,. \tag{3.28}$$

4. Results

Equation (3.10) has been employed in the calculation of some resonant frequencies of two plano-convex resonators, which are compared with frequency measurements on the respective resonators. The first resonator has a blank diameter of .550 in., an electrode diameter of .370 in., a radius of curvature R of 5 diopters, which is 106 mm, an electrode mass loading ratio R of 1.864×10^{-3}

and a measured thickness $2h_o = .0271$ in. $= .6883$ mm. Since we did not have confidence in the accuracy of the measured thickness to the required number of significant figures, we adjusted the thickness in order that the calculated value of f(3,0,0) agree with the measured value. The adjusted thickness $2h_o$ is .68785 mm. The comparison between the calculated and measured values is given in Table I, which shows that the agreement between theory and experiment is excellent with the exception of f(1,2,2). We believe that strong coupling to flexure, which has been omitted from the theory, exists in the case of the mode for which the calculation does not agree well with the measurements. The measured frequencies in Table I are the average values determined from five units. For this resonator the motional capacitances of a few of the modes have been calculated from Eq. $(3.27)_2$ and compared with the average value determined from the measurement of five units for each mode. The comparison between the calculated and measured values is given in Table II, which shows that the agreement between theory and experiment is reasonably good.

The second resonator has a blank diameter of .590 in., an electrode diameter of .374 in., a radius of curvature R of 2.0 in., which is .0508 m, a measured thickness of gold electrode $2h' = 750$ Å and a maximum plate thickness $2h_o = .06502$ in. $= 1.6515 \times 10^{-3}$ m. In this case we used the measured maximum plate thickness, since the measurement is considered to be accurate to one more significant figure than in the case of the first resonator, and consequently, no adjustable parameters were employed. The comparison between the calculated and measured values is given in Table III, in which excellent agreement between theory and experiment is indicated again.

Acknowledgements

We wish to thank Drs. T.R. Meeker and A.A. Comparini of Bell Laboratories for providing the measured data associated with Table III.

The work of one of the authors (HFT) was supported in part by the Army Research Office under Grant No. DAAG29-76-G-0176 and the Office of Naval Research under Contract No. N00014-76-C-0368.

REFERENCES

1. H.F. Tiersten, "Analysis of Trapped Energy Resonators Operating in Overtones of Coupled Thickness-Shear and Thickness-Twist," J. Acoust. Soc. Am., 59, 879 (1976).

2. C.J. Wilson, "Vibration Modes of AT-Cut Convex Quartz Resonators," J. Phys. D: Appl. Phys., 7, 2449 (1974).

3. H.J. McSkimin, in Quartz Crystals for Electrical Circuits, edited by R.A. Heising (D. Van Nostrand, New York, 1946), Chap.VII.

4. W.G. Stoddard, "Design Equations for Plano-Convex AT Filter Crystals," Proceedings of the 17th Annual Symposium on Frequency Control, U.S. Army Electronics Command, Fort Monmouth, New Jersey, 272 (1963).

5. H.F. Tiersten, "Analysis of Intermodulation in Thickness-Shear and Trapped Energy Resonators," J. Acoust. Soc. Am., 57, 667 (1975).

6. P.M. Morse and H. Feshbach, Methods of Theoretical Physics, Part I (McGraw-Hill, New York, 1953), Chap.6.

7. Ref.7, p.786.

TABLE I

Mode N M P	Calculated Frequency kHz	Measured Frequency kHz
1 0 0	2508.2	2505.5
1 0 2	2684.0	2683.4
1 2 0	2728.6	2727.7
1 2 2	2891.0	2843.2
3 0 0	7325.8	7325.8
3 0 2	7510.9	7514.1
3 2 0	7520.0	7520.1
3 2 2	7700.5	7693.4
5 0 0	12152.6	12154.1
5 0 2	12339.6	12343.0
5 2 0	12366.3	12367.7
5 2 2	12550.1	12532.0

TABLE II

Mode N M P	Calculated C_1 fF	Measured C_1 fF
1 0 0	14.24	13.21 ± .05
1 0 2	5.81	6.25 ± .24
1 2 0	4.64	2.16 ± .03
3 0 0	0.50	0.52 ± .03

TABLE III

Mode N M P	Calculated Frequency kHz	Measured* Frequency kHz
1 0 0	1097.47	1094.75
1 0 2	1248.72	1245.93
1 2 0	1285.69	1263.23
1 2 2	1416.99	-
3 0 0	3103.25	3103.54
3 0 2	3270.74	3278.93
3 2 0	3278.82	3285.67
3 2 2	3437.77	3430.30
5 0 0	5123.38	5120.14
5 0 2	5294.40	5297.28
5 2 0	5318.61	5319.72
5 2 2	5483.54	5472.17
7.0 0	7127.01	7129.09
7 0 2	7299.73	7292.75
7 2 0	7318.23	7320.40
7 2 2	7486.54	7486.37

* Mode identification is conjectural. Measured data courtesy of T.R. Meeker and A.A. Comparini of Bell Laboratories.

FIGURE CAPTIONS

Figure 1	Plano-convex Resonator
Figure 2	Electroded Flat Plate
Figure 3	Geometry for Spherically Contoured Surface of Resonator

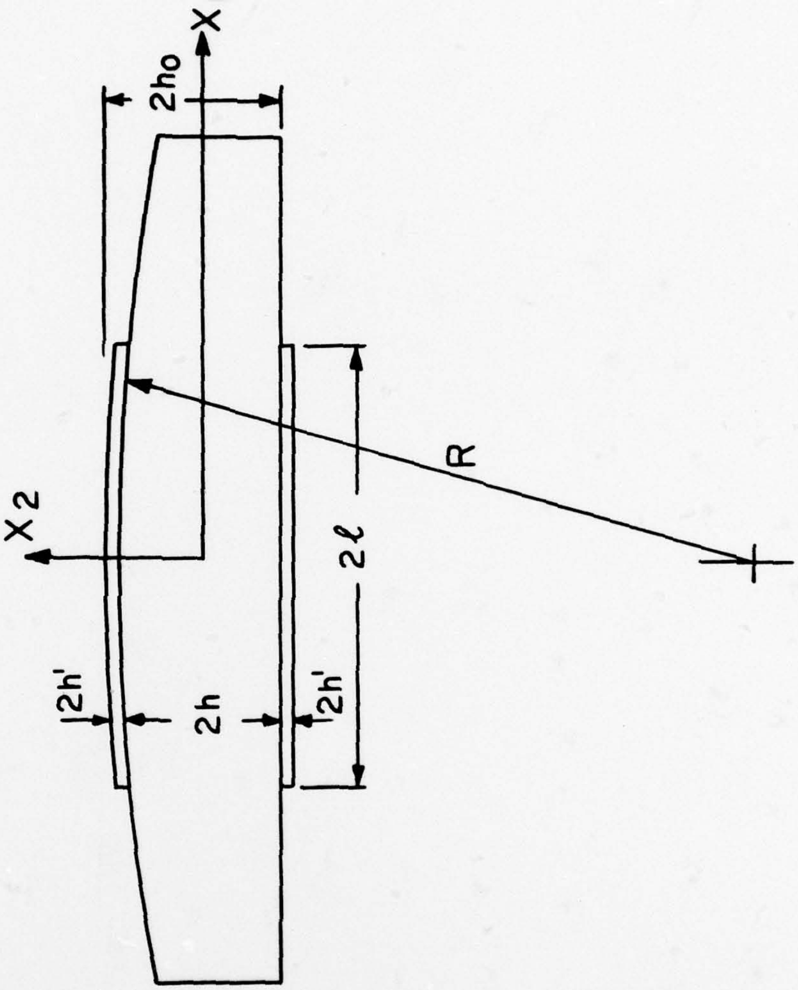

Fig. 1

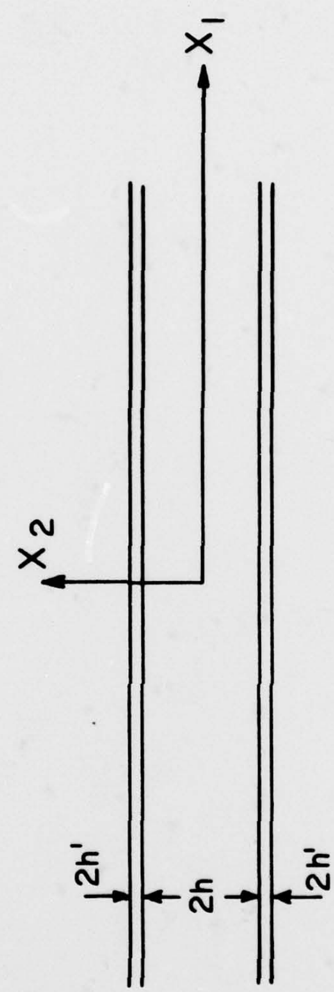

Fig. 2

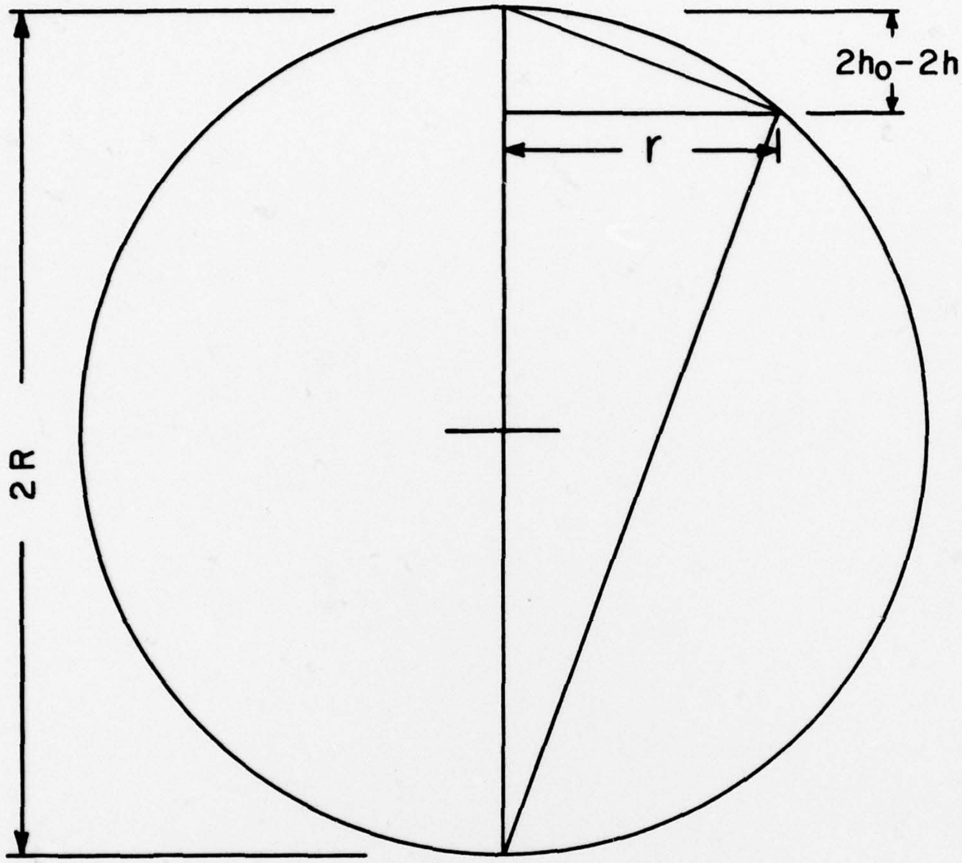

Fig. 3